DNA Duplex-Based Photodynamic Molecular Beacon for Targeted Killing of Retinoblastoma Cell

Yanchun Wei,[1,2] Cuixia Lu,[1] Qun Chen,[1] and Da Xing[1,3]

[1]MOE Key Laboratory of Laser Life Science & Institute of Laser Life Science, College of Biophotonics South China Normal University, Guangzhou, People's Republic of China
[2]Jiangsu Provincial Key Laboratory for Interventional Medical Devices, Huaiyin Institute of Technology, Huan'an, China
[3]Joint Laboratory of Laser Oncology with Cancer Center of Sun Yat-sen University, South China Normal University, Guangzhou, China

Correspondence: Qun Chen, MOE Key Laboratory of Laser Life Science & Institute of Laser Life Science, College of Biophotonics South China Normal University, Guangzhou 510631, P. R. China;
chenqun@scnu.edu.cn.
Da Xing, MOE Key Laboratory of Laser Life Science & Institute of Laser Life Science, College of Biophotonics South China Normal University, Guangzhou 510631, P. R. China;
xingda@scnu.edu.cn.

Submitted: November 23, 2015
Accepted: September 14, 2016

Citation: Wei Y, Lu C, Chen Q, Xing D. DNA duplex-based photodynamic molecular beacon for targeted killing of retinoblastoma cell. *Invest Ophthalmol Vis Sci*. 2016;57:6011–6019. DOI:10.1167/iovs.15-18723

Purposes. Retinoblastoma (RB) is the most common primary intraocular malignancy of infancy. An alternative RB treatment protocol is proposed and tested. It is based on a photodynamic therapy (PDT) with a designed molecular beacon that specifically targets the murine double minute x (MDMX) high-expressed RB cells.

Methods. A MDMX mRNA triggered photodynamic molecular beacon is designed by binding a photosensitizer molecule (pyropheophorbide-a, or PPa) and a black hole quencher-3 (BHQ3) through a complementary oligonucleotide sequence. Cells with and without MDMX high-expression are incubated with the beacon and then irradiated with a laser. The fluorescence and reactive oxygen species are detected in solution to verify the specific activation of PPa by the perfectly matched DNA targets. The cell viabilities are evaluated with CCK-8 and flow cytometry assay.

Results. The fluorescence and photo-cytoxicity of PPa is recovered and significantly higher in the MDMX high-expressed Y79 and WERI-Rb1 cells, compared to that with the MDMX low-expressed cells.

Conclusions. The synthesized beacon exhibits high PDT efficiency toward MDMX high-expressed RB cells. The data suggest that the designed beacon may provide a potential alternative for RB therapy and secures the ground for future investigation.

Keywords: photodynamic molecular beacon, retinoblastoma, mRNA targeting

Retinoblastoma is the most common primary intraocular malignancy of infancy and is virtually fatal if left untreated due to metastasis. The current therapies include radical enucleation and conservative treatments such as local thermotherapy, cryotherapy, brachytherapy or chemotherapy.[1–3] The effectiveness of the treatments is significantly limited due to the delicate anatomical structure of the site and potential late effects. Here lies the need of improved therapies that specifically target retinoblastoma cells while preserving the healthy ocular tissue structure.

There are two major pathways in cell death, necrosis and apoptosis.[4] Necrosis is a traumatic cell death that involves minimal autoregulation and is often associated with severe immune responses such as inflammation, swelling, and pain, and is to be avoided in retinoblastoma therapies in general. Apoptosis is a process of programmed cell death. It is initiated either intrinsically due to cellular stress or extrinsically when receiving signals from other cells. It is part of a typical lifecycle of organism with no traumatic symptoms related to the process. Given the delicate anatomical structure, apoptosis is a preferred cell killing mechanism for treating retinoblastoma.

Photodynamic therapy (PDT) with the photosensitizer Visudyne has been approved by the US Food and Drug Administration for treatment of age-related macular degeneration. It has been suggested that the therapeutic mechanism may also be useful for various ocular tumors, such as retinoblastoma, choroidal hemangioma, and retinal astrocytoma.[5–8] With preadministered photosensitizers, PDT can destroy target cells when light activates the drug to generate cytotoxic reactive oxygen species (ROS), mainly singlet oxygen ($^1O_2$).[9–11] However, despite the many advantages of PDT over conventional treatments, development of selective PDT agents to improve therapeutic efficiency and reduce side effects remains a significant challenge.[12–15]

The extent of PDT cytotoxicity can be controlled by the irradiation light "dosage." Furthermore, PDT treatment can be repeated as necessary with minimal side effects or multidrug resistance. It is thus possible, by controlling the PDT dose and using target-specific molecular beacon, to selectively induce apoptosis in the retinoblastoma cells for therapeutic purpose.

Tumors are associated with abnormal gene expression. Laurie et al.[16] showed that retinoblastoma selectively amplifies murine double minute x (MDMX),[16,17] an antagonist of p53. The aberrant expression leads to an inactivation of the p53 pathway via the formation of inactive p53-MDMX complexes, contributing to the development and progression of retinoblastoma formation.[18] Murine double minute x expression level is closely correlated with MDMX mRNA level and MDMX promoter activity in different tumor cell lines.[19] Murine double minute x was identified as a therapeutic target for p53

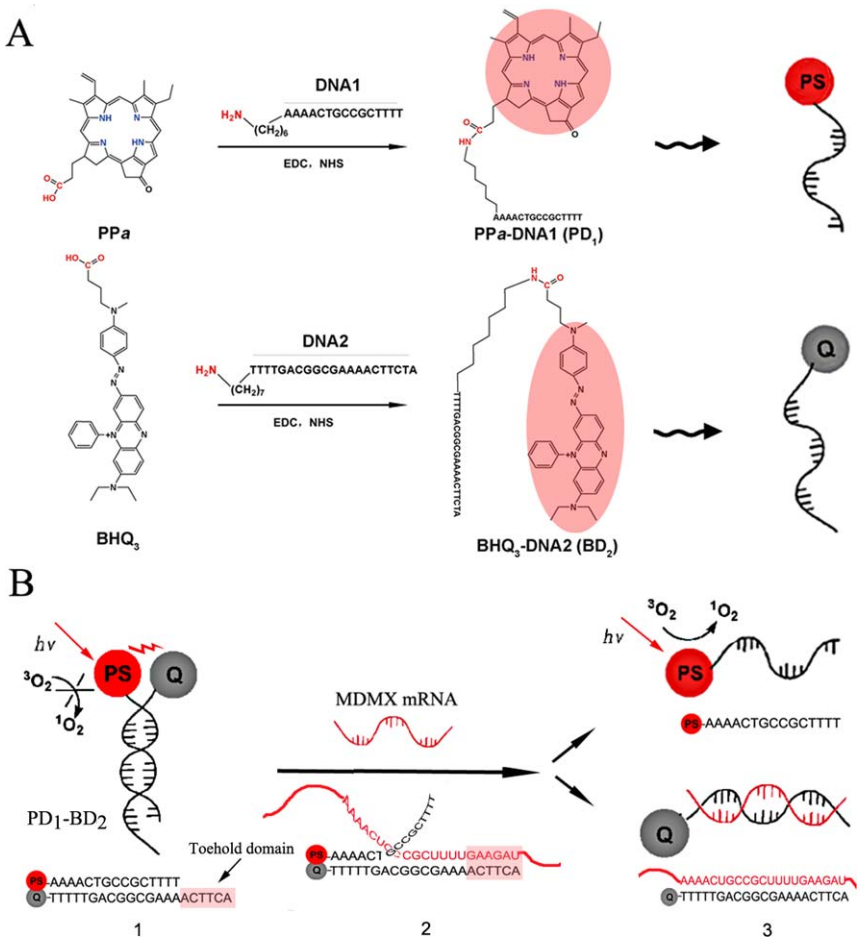

FIGURE 1. Synthesis of photodynamic molecular beacon and its $^1O_2$ generation triggered by MDMX mRNA. (**A**) Synthesis protocols of PPa-DNA1 (PD_1) and BHQ_3-DNA2 (BD_2). (**B**) Schematic of the beacon triggered by MDMX mRNA. (1) The formed PD_1-BD_2 with photosensitizer (PS) quenching; (2) MDMX mRNA binds to PD_1-BD_2 through a single-strand toehold domain; (3) PS switched on to yield $^1O_2$ after the displacement reaction.

reactivation in tumors, especially, as a chemotherapeutic target for the treatment of retinoblastoma.[17] Nutlin-3 is the currently available MDMX inhibitor. It can block the MDMX–p53 interaction. However, its affinity to MDMX is low.[16,20,21] Systemic administration of Nutlin-3 to treat the tumors with MDMX high-expression is not feasible due to its pharmacokinetics and toxicity in multiple organs.[22]

Zheng et al.[23–26] introduced a hairpin-based photodynamic molecular beacon. It comprises a tumor-specific linker, a photosensitizer, and a $^1O_2$ quencher. The photoactivity of the photosensitizer is silenced until the linker interacts with a target molecule, protease,[23–26] or RNA.[27,28] This strategy minimizes the cytotoxicity and organs toxicity of the drug to the none-target tissue, and thus may be particular advantage for treating ocular tumors. Clo et al.[29] designed a DNA duplex-based photodynamic molecular beacon that can be selectively triggered by oligonucleotides hybridization ex vivo[28–30] by means of Watson–Crick base pairing. The photosensitizer and the quencher are kept in close proximity in the "off state" based on FRET (fluorescence resonance energy transfer) effect by DNA-programmed assembly. To switch the photosensitizer "on," a more complementary strand is introduced to hybridize with the quencher moiety and causes photosensitizer moiety release, allowing a restoration of the $^1O_2$ production. In addition, the $^1O_2$ luminescence recovery efficiency of DNA duplex-based photodynamic molecular beacons is higher than that of traditional hairpin-based photodynamic molecular beacons.[31] Recently, a zipper molecular beacons based on the similar mechanism has also been proposed.[32] These approaches enhance the target selectivity in PDT over its intrinsic targeting mechanism.

In this study, to selectively destroy retinoblastoma cells, we designed a DNA duplex-based MDMX mRNA triggered photodynamic molecular beacon based on the amplification of MDMX gene expression in retinoblastoma for PDT (Fig. 1). The designed beacon is hybridized with two complementary DNA sequences (Fig. 1A). A formed toehold domain is used to initiate the displacement reaction of the MDMX mRNA and the beacon. The reaction would open the duplex DNA strand to trigger the photosensitizer molecular on (Fig. 1B). As the first step of implementing the beacon as a therapeutic strategy for retinoblastoma treatment, we validate the targeting effect of MDMX mRNA-triggered photodynamic molecular beacon to retinoblastoma cells, and the PDT effect in vitro.

MATERIALS AND METHODS

Chemicals and Reagents

The following chemicals and reagents were used in our experiments: pyropheophorbide-a (PPa) (J&K Scientific Ltd, Nanjing, Jiangsu, China), BHQ-3 Carboxylic Acid (Biosearch Technologies, Inc., Navato, CA, USA), CCK-8 (Dojindo Laboratories, Kumamoto, Japan), fluoresceinyl cypridina luciferin

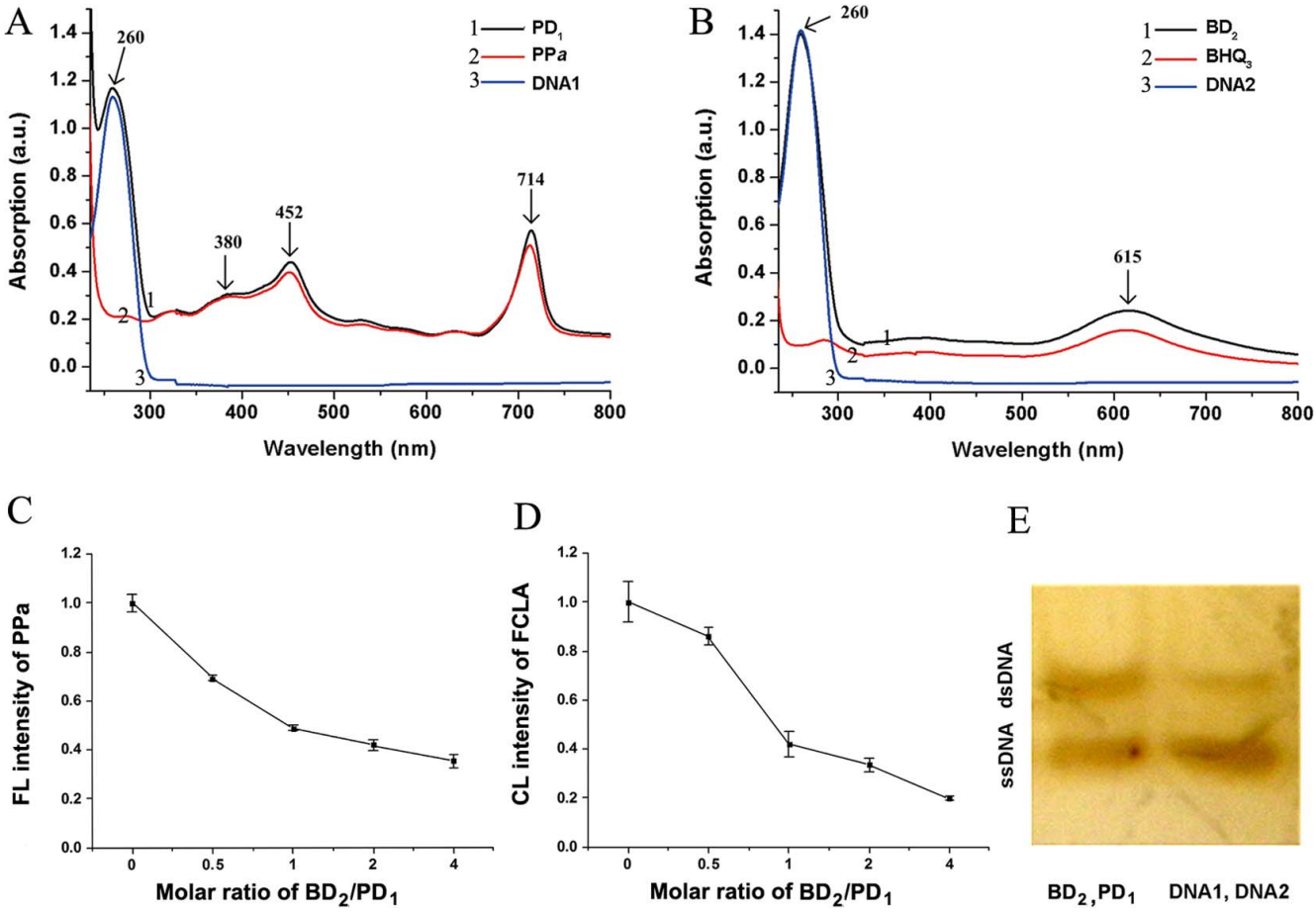

FIGURE 2. Confirmation and characterization of PD_1-BD_2. (**A**, **B**) UV-VIS absorption spectra demonstrating the specialized PD_1 and BD_2 each possess the corresponding characterization of their building blocks. (**C**, **D**) PPa quenching shown as fluorescence (FL) and ROS production (n = 3). The FL intensity was measured with 488-nm excitation and normalized to that of PD_1 only (**C**). Reaction oxygen species production was evaluated with FCLA chemiluminescence (CL) (**D**). (**E**) Native polyacrylamide gel electrophoresis and silver stain of PD_1 with BD_2, and DNA1 with DNA2.

analog (FCLA) (Tokyo Kasei Kogyo Co., Tokyo, Japan), Lipofectamine 2000 reagent (Invitrogen, Carlsbad, CA, USA), N-Hydroxysuccinimide (NHS), and 1-ethyl-3-(3-(dimethylaminopropyl)carbodiimide (EDC) (Sigma-Aldrich Corp., St. Louis, MO, USA). All the reagents were of analytical grade and used without further purification. Deionized water was used throughout.

Preparation and Characterization of PD_1-BD_2

Synthesis of PPa-DNA1 (PD_1) and BHQ3-DNA2 (BD_2). To synthesize PD_1, stock solution of PPa (1 mM) was prepared in DMSO (dimethyl sulfoxide). Labeling buffer (100 mM sodium carbonate, pH 7.5) was prepared by dissolving an appropriate amount of sodium carbonate in water and its pH titrated with HCl and/or NaOH. A 15mer-oligonucleotide (DNA 1) modified with amino groups at the 5′ end was obtained from Invitrogen. The oligonucleotide was dissolved in the labeling buffer to yield a 100-μM solution. The reaction mixture included (in order of addition): labeling buffer (162 μL), PPa (60 μL), EDC (12 μL, 100 mM), NHS (6 μL, 100 mM), and DNA 1 (60 μL, 6 nmol). The reaction mixture was incubated at the room temperature overnight and then purified with dialysis. To detect the intrinsic optical properties of PD_1, ultraviolet-visible (UV-VIS) spectrum was performed. The similar synthesis process was performed for BD_2 by using BHQ3 (42 μL,1.44 mM), 21mer-oligonucleotide (DNA2) (60 μL, 6 nmol), and labeling buffer (180 μL). The sequence of DNA1 and DNA2 were 5′-AAAACTGCCGCTTTT-3′ and 5′-ATCTTCAAAAGCGGCAGTTTT-3′, respectively.

To hybridize the complementary strands, PD_1 (10 μL, 10 μM) and BD_2 (10 μL, 10 μM) in 100 mM sodium carbonate (pH 7.5) were heated in a thermocycler at 95°C for 5 minutes and cooled slowly to 5°C (2°C per minute). To characterize the duplex DNA complex, quenching efficiency of fluorescence and ROS production from PD_1 was measured. PD_1 with a fixed concentration 1 μM was mixed with BD_2 solutions at different concentration (0.5, 1, 2, 4 μM), then hybridized. Reactive oxygen species production was measured by the basic PDT chemiluminescence measurement system, which is based on measurement of chemiluminescence from FCLA when activated by PDT-generated ROS.[33,34] The chemiluminescence (532 nm) from FCLA was measured with 633-nm light excitation. The background was subtracted and the data were normalized relative to PD_1. The fluorescence spectra of PD_1 were obtained using an LS-55 fluorescence spectro-photometer (Perkin-Elmer, Waltham, MA, USA) with an excitation of 488 nm. The data of the fluorescence intensity were normalized relative to PD_1.

Gel electrophoresis was used to confirm the synthesis of PD_1-BD_2. PD_1 (10 μL, 10 μM) and BD_2 (20 μL, 10 μM) were hybridized. DNA 1 (10 μL, 10 μM) and DNA 2 (20 μL, 10 μM) were hybridized to serve as positive control. Ten microliters of each hybridization production was loaded onto a 10% native

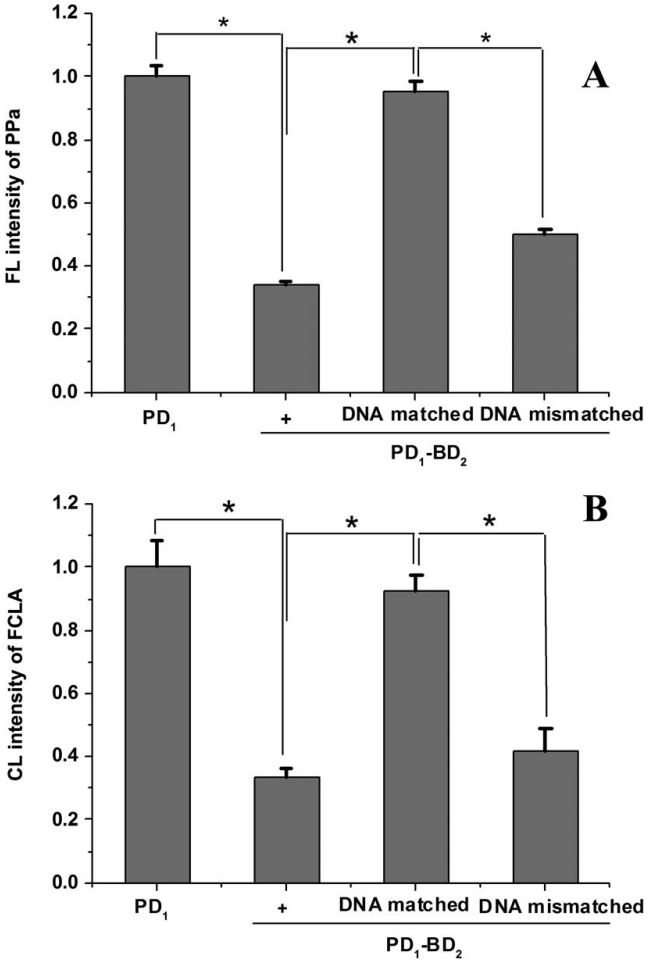

FIGURE 3. Recovery efficiency of PD_1-BD_2 after DNA sequence targeting. The recovered fluorescence emission (**A**) and ROS production (**B**) of PD_1-BD_2 by mixing with matched or single-base mismatched DNA targets. PD_1 was used as a positive control. $^*P < 0.05$ ($n = 3$).

polyacrylamide gel (29:1 acryl/bisacryl) in 1× Tris-borate-EDTA (TBE). Gels were run at room temperature for 1 hour at 120 V. The gel was conducted with silver staining and photographed by a Nikon 4500 digital camera.

The Specificity Activation of PD_1-BD_2 in Solution

A short 21mer-nucleotide sharing the complementary sequence of the DNA2 (DNA target 1) and a short 21mer-nucleotide with single-base mismatch (DNA target 2) were synthesized (5′-AAAACTGCCGCTTTTGAAGAT-3′ and 5′-AAAACTGTCGCTTTTGAAGAT-3′). PD1-BD2 with a fixed concentration at 1 μM was mixed with the perfectly matched DNA (10 μM) and single-base mismatched DNA (10 μM). Reactive oxygen species production was measured by FCLA chemiluminescence with 633-nm excitation wavelength. The fluorescence intensity of PPa was measured with 488-nm excitation wavelength.

Cell Line and Transfection

The human retinoblastoma cell lines Y79 and WERI-Rb1 were cultured in RPMI-1640 Medium (1640, GIBCO, Grand Island, NY, USA) supplemented with 10% fetal calf serum (FCS) in 5% CO_2, 95% air at 37°C in a humidified incubator. D407 (human retinal pigment epithelium cell line) cells were cultured with DMEM supplemented with 5% fetal bovine serum (FBS) in a humidified atmosphere of 5% CO_2 at 37°C.

Gene Silencing. For gene silencing in Y79 and WERI-Rb1 cells, we used MDMX shRNA and negative control shRNA. pGPU6/GFP/Neo vector carrying MDMX shRNA (5′-GTGAT GATACCGATGTAGA-3′) and nonsense sequence shRNA (negative control) (5′-GTTCTCCGAACGTGTCACGT-3′) were synthesized and constructed by Shanghai GenePharma Company (China).

When the cells grew to 70% to 80% confluence, transfection was performed with 0.8 μg shMDMX using the Lipofectamine 2000 according to the manufacturer's instructions in serum-free medium. The serum-free medium was replaced with fresh culture medium 5 hours after and the cells were incubated for an additional 24 to 48 hours for expression. D407 cells, as a control, were also subjected to the same process.

Total RNA Extraction and Semiquantitative RT-PCR. To determine the level of MDMX expression in Y79, WERI-Rb1, and D407 cells, as well as their MDMX-knockdown ones, total RNA was extracted from the cells (2×10^6 cells mL^{-1}) according to the manufacturer's instructions using the TRI reagent (Sigma-Aldrich Corp.). The RNA concentrations were determined by measuring the corresponding optical densities (OD) at 260 nm. First-strand cDNA was synthesized with the SuperScript II First-Strand Synthesis System for RT-PCR (Invitrogen). The primers used for semiquantitative RT-PCR of human MDMX mRNA were as follows: human MDMX, forward (FW), 5′-GCCTTGAGGAAGGATTGGTA; reverse (REV), 5′-TCGACAATCAGGGACATCAT; human GAPDH, FW, 5′-ACCA CAGTCCATGCCATCAC; REV, 5′-TCCACCACCCTGTTGCTGTA.

The murine double minute x level in Y79 was also assessed with the similar process to determine the reaction capability of PD_1-BD_2 with MDMX mRNA after the cells were incubated with PD_1-BD_2, MDMX shRNA, and DNA2.

PD_1-BD_2 Triggered by MDMX mRNA in Living Cell

Cancer cells (1×10^4 per well) growing in 35-mm Petri dishes were incubated with the targeting PD_1-BD_2 probe for 4 hours. After being centrifuged, the cells were rinsed with PBS and replaced with fresh cell medium. The cells were imaged by a commercial laser scanning microscope (LSM 510/ConfoCor 2, combination system Zeiss, Jena, Germany) equipped with a Plan-Neofluar 40×/1.3 NA Oil DIC objective. The targeting probe was excited at 633 nm, and its fluorescence emission was recorded through a 650- to 700-nm IR band-pass filter.

Quantification of Fluorescence Intensity

Flow cytometry was used to quantitatively assess fluorescence intensity of PD_1-BD_2 in cells. Y79, WERI-Rb1, and their shMDMX cells were incubated with PD_1-BD_2 and PD_1 in a 12-well microplate for 4 hours. The cells were centrifuged and washed, then resuspended in ice-cold PBS. The fluorescence histogram of cells in different treatments was obtained from 10,000 cells with flow cytometry (FACScan, Becton Dickinson, Mountain View, CA, USA).

Photodynamic Treatment and Cell Viability

To test the phototoxicity of PD_1-BD_2, the cell viability was evaluated with CCK-8 assay (Dojindo Molecular Technologies, Inc., Kumamoto, Japan). Y79 cells were incubated with the PD_1-BD_2 samples at various concentrations (PPa, 0.2∼0.6 μM) in a 96-well microplate (six wells per group) at 37°C under 5% CO_2 /95% air for 4 hours. Then, the mixtures were washed three times with PBS to remove PD_1-BD_2 in the solution. The tumor cells were irradiated with a 633-nm laser (30 J cm^{-2}

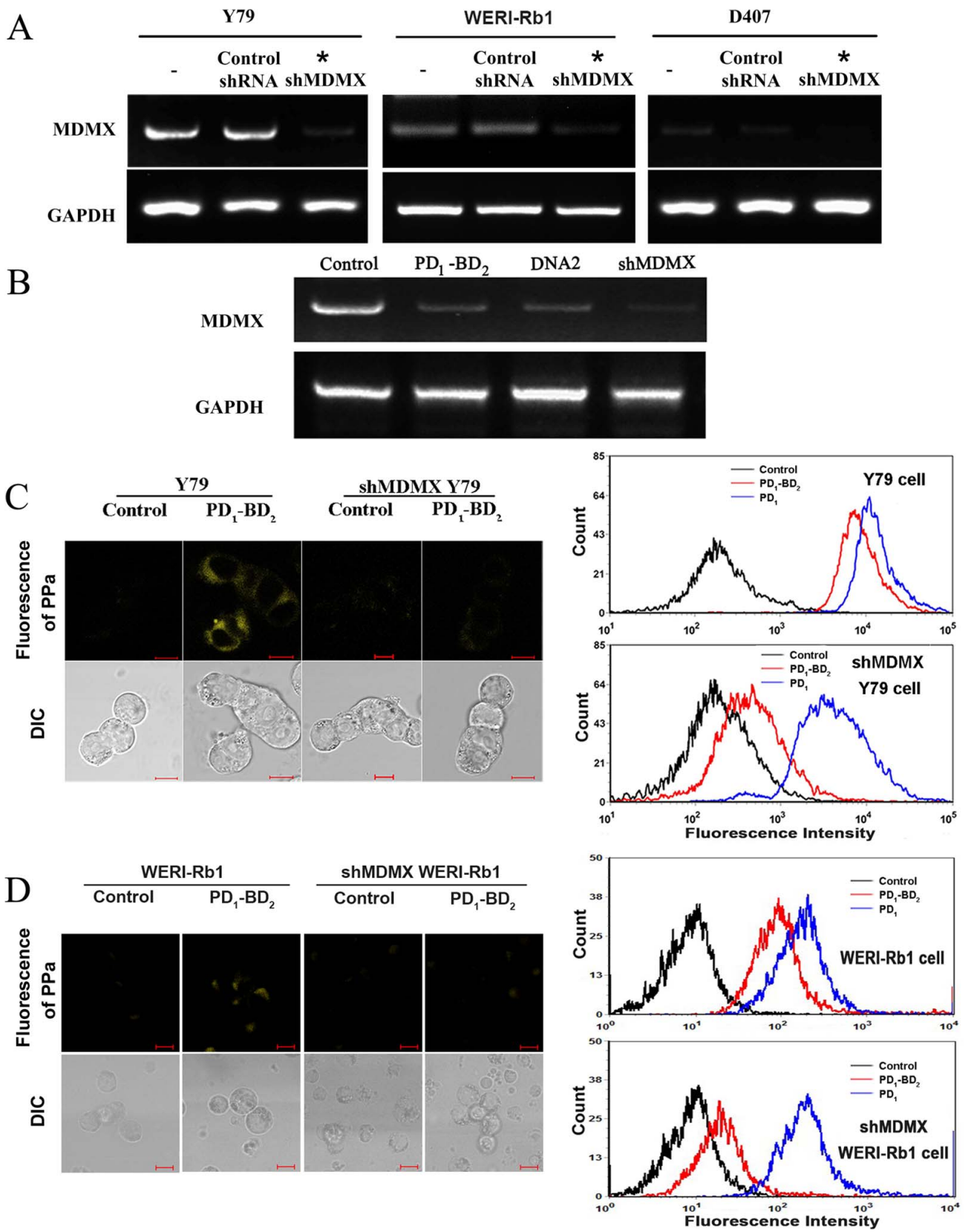

FIGURE 4. Expression of MDMX mRNA and its specificity of PD_1-BD_2. (**A**) The expressions of MDMX mRNA in Y79, WERI-Rb1, and D407 cells were measured with RT-PCR after the cells were conducted with null, negative (Control shRNA), and positive (shMDMX) MDMX knockdown. The * indicates the significant difference of shMDMX group with its control. $^*P < 0.05$ ($n = 3$). (**B**) The murine double minute x mRNA knockdown effect of PD_1-BD_2 in Y79 cells by comparing with the control, DNA2, and shMDMX Y79. (**C**, **D**) MDMX mRNA specificity of PD_1-BD_2 in Y79 and WERI-Rb1 cells. *Left*, confocal imaging of MDMX positive and negative cells. *Right*, fluorescence histogram of cells incubated with PD_1-BD_2 and PD_1 detected by flow cytometry. *Scale bars* in **C** and **D**: 10 μm.

Investigative Ophthalmology & Visual Science

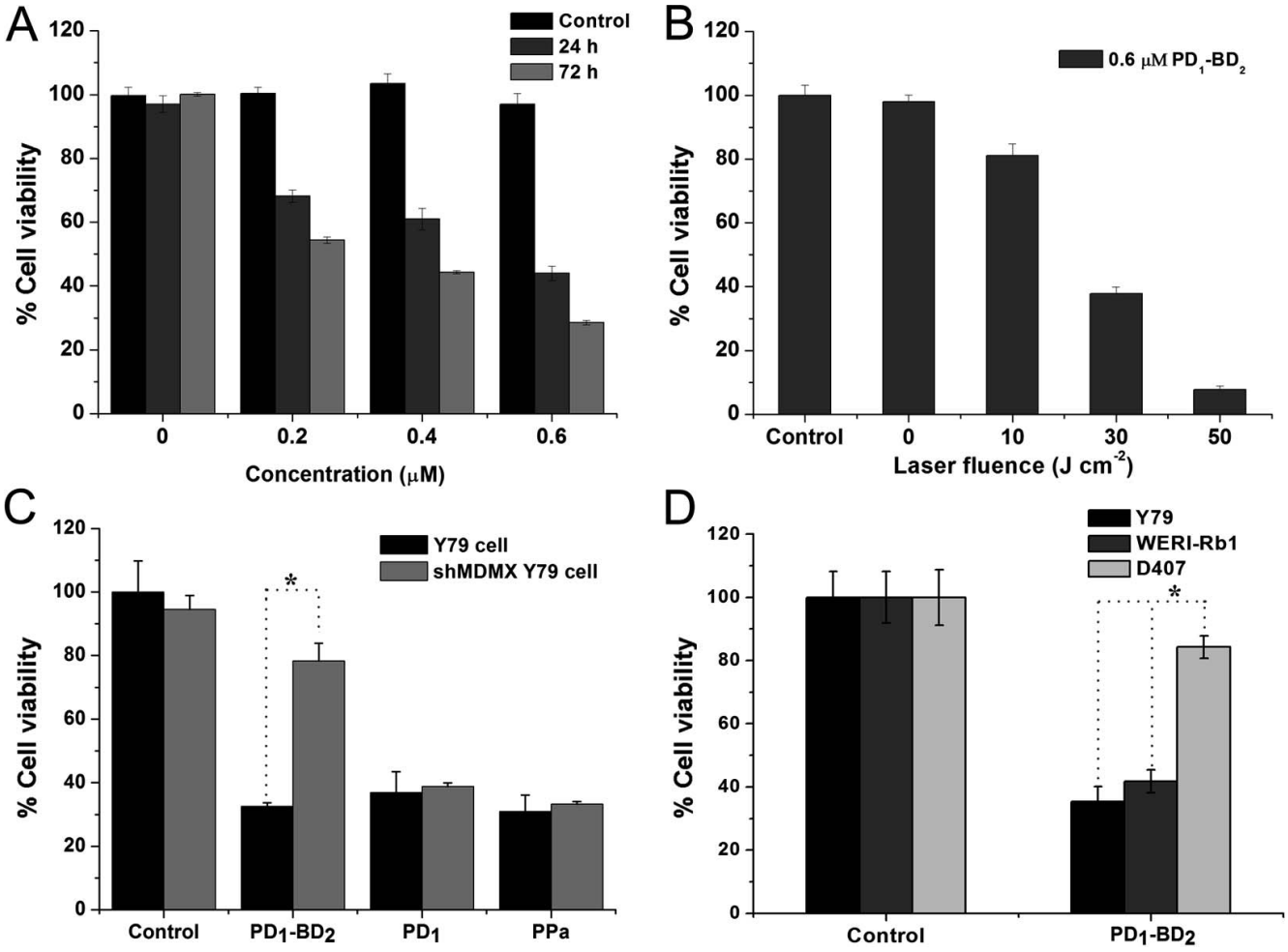

FIGURE 5. The viability of cells under different treatments. (**A**) Y79 cells were incubated with different doses of PD_1-BD_2 (0, 0.2, 0.4, and 0.6 μM), and assessed at 24 and 72 hours after 30 J cm^{-2} laser irradiation. (**B**) Y79 cells were incubated with 0.6 μM PD_1-BD_2 and irradiated with different laser fluence. (**C**) Y79 and shMDMX Y79 cells were incubated with PD_1-BD_2, PD_1, and PPa (0.6 μM), followed by laser irradiation (30 J cm^{-2}). (**D**) Y79, WERI-Rb1, and D407 cells were incubated with PD_1-BD_2, and followed by laser irradiation (30 J cm^{-2}). *$P < 0.05$.

over 5 minutes). Cell cytotoxicity was assessed with CCK-8 24 and 72 hours after the laser irradiation. Y79 cells were also incubated with 0.6 μM PD_1-BD_2 and irradiated with various laser fluence (10, 30, and 50 J cm^{-2}), then assessed with CCK-8 24 hours after the laser irradiation. OD: the absorbance value at 450 nm was read with a 96-well plate reader (INFINITE M200, Tecan, Switzerland), to determine the viability of the cells.

Y79 and shMDMX Y79 cells were incubated with PD_1-BD_2, PD_1, and PPa samples at 0.6 μM PPa concentration in a 96-well microplate for 4 hours. Cell viability was assessed with CCK-8 48 hours after laser irradiation. With the similar protocol, the cell viabilities of Y79, WERI-Rb1, and D407 were also assessed after the PD_1-BD_2 incubation.

Flow Cytometry Experiments for the Apoptosis of Cancer Cells

Quantitation of apoptosis and necrosis by Annexin V/PI staining was performed. The Y79 cells and WERI-Rb1 cells with different treatments were collected after 24 hours post PDT. Apoptotic cell death was determined using the BD ApoAlert annexin V-FITC Apoptosis Kit (Becton Dickinson, Biosciences) according to the manufacturer's instructions, with a BD FACS Canto TM II flow cytometer (Becton Dickinson).

Statistical Analysis

Data are presented as means ± SD from at least three experiments. One-way ANOVA is used to compare the treatment effects. $P < 0.05$ is considered statistically significant.

Results and Discussion

PD_1-BD_2 Preparation and Its Characterization Analysis

The two molecular building blocks, PD_1 and BD_2, were synthesized as shown in Figure 1A. The outcomes were then verified by their UV-VIS absorptions (Figs. 2A, 2B). In the PD_1-BD_2 preparation, the freshly synthesized PD_1 and BD_2 would be hybridized to form the complementary strands. To study the quenching efficiency of BD_2 on PPa due to the hybridization, BD_2 was titrated up to 4-fold in Mole concentration excessive that of PD_1. The fluorescence and ROS generation of PPa were then detected and compared. As shown in Figure 2C, when the concentration ratio of BD_2/PD_1 increased to 2, the fluorescence emission from PD_1 was reduced to 41.7% ± 2.3% of the initial

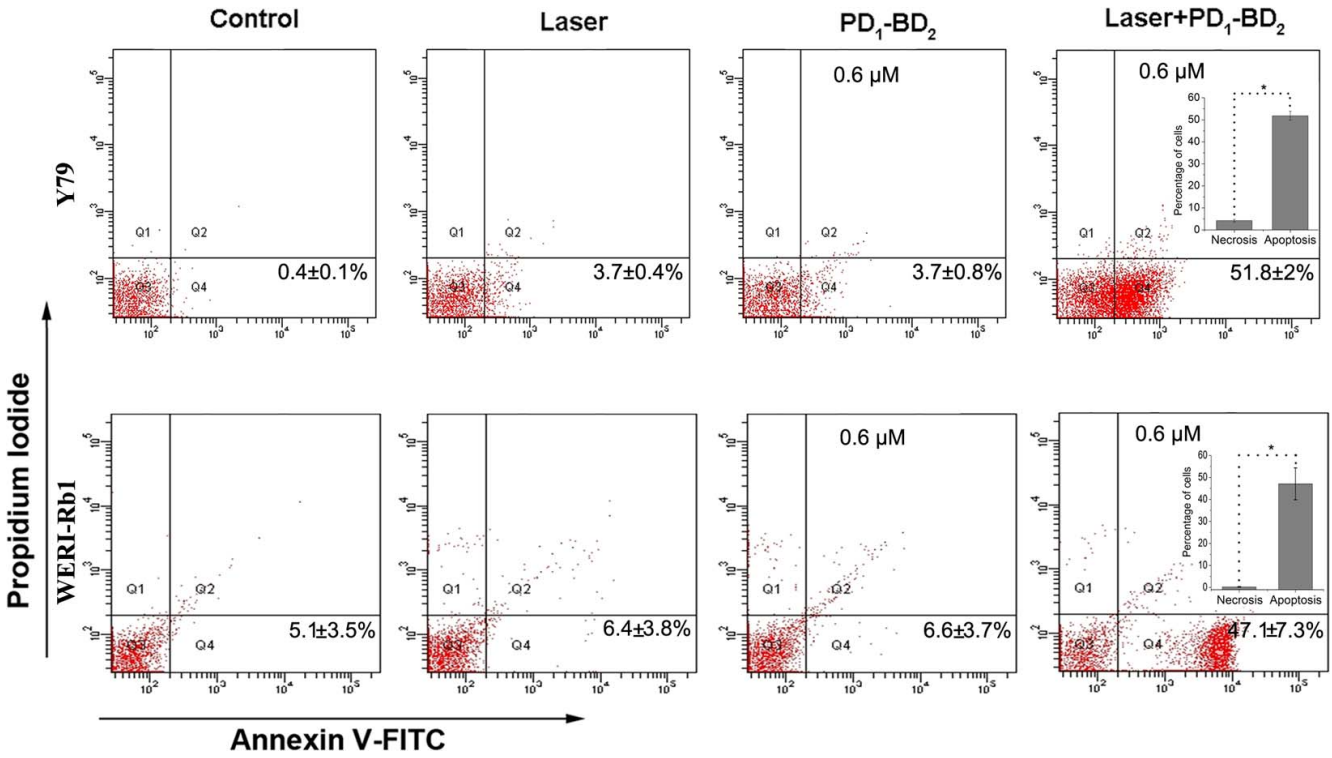

FIGURE 6. Cell apoptosis analysis. Cell apoptosis of Y79 and WERI-Rb1 cells under different treatment protocols were analyzed with FACS. The averaged percentage of cell apoptosis is marked. The inserted histograms show the percentage of cell necrosis and apoptosis in PDT. Y79 and WERI-Rb1 cells were incubated with PD_1-BD_2 (0.6 μM), followed by 30 J cm^{-2} laser irradiation ($n = 3$).

value. A similar trend was observed in the quenching of PD_1 ROS generation (Fig. 2D). Reaction oxygen species generation was evaluated with FCLA by using its emission at 532 nm. In the presence of two folds of BD_2, the ROS production from PD_1 was reduced to 33.6% ± 2.8% of the initial value.

To further confirm the hybridization of PD_1 and BD_2, polyacrylamide gel electrophoresis (PAGE) was performed (Fig. 2E). The upper band of left lane indicates that the two strands of PD_1 and BD_2 has formed duplex after hybridization, while the lower band presents excess PD_1 and BD_2. The right lane is a positive control in which a corresponding free DNA was used at the same molar ratio. These results suggest that the hybridization of PD_1 and BD_2 forced PPa and BHQ3 into close contact, attenuating the singlet oxygen signal and fluorescence of PPa.

PD_1-BD_2 was synthesized by PD_1 and BD_2 hybridization. To verify the gene-specific activation of PD_1-BD_2 by MDMX mRNA, the synthesized DNA target 1 and DNA target 2 were titrated to PD_1-BD_2. The resulting fluorescence intensity and ROS production were measured. Initially, the fluorescence intensity of PD_1-BD_2 was significantly less than that of PD1 ($P < 0.05$), but increased significantly (278% ± 10%) when hybridized with the perfectly matched DNA ($P < 0.05$). In comparison, only a 46% ± 5% increase was achieved with the single-base mismatched DNA (Fig. 3A). By using a 633-nm laser to irradiate the PD_1 and PD_1-BD_2, the ROS production was measured. A similar result with fluorescence was observed: the MDMX matched DNA strands significantly recovered the ROS producing of PD_1-BD_2 (Fig. 3B). These results suggest that PD_1-BD_2 was specific and sensitive to the matched DNA target.

PD_1-BD_2 Triggered by MDMX mRNA in Living Cell

The MDMX mRNA expression and the mRNA knockdown efficiency of Y79, WERI-Rb1, and D407 cells were evaluated with the RT-PCR method (Fig. 4A). It shows that the Y79 and WERI-Rb1 cells had significantly higher MDMX mRNA expression, compared to that in shMDMX and D407 cells. The latter were then used as the negative controls. The knockdown efficiencies of the Y79 and WERI-Rb1 cells were 86% ± 2% and 77% ± 1.4%, respectively. The reaction capability of PD_1-BD_2 with MDMX mRNA was also assessed by comparing with DNA2 and MDMX shRNA in Y79 cells. The result (Fig. 4B) indicates that, through the hybridization reaction with MDMX mRNA, the PD_1-BD_2 reduced the mRNA level.

To confirm whether the photodynamic beacon can be specifically activated by MDMX mRNA in cancer cells, Y79 and WERI-Rb1 cells were incubated with PD_1-BD_2. The cells with high MDMX expression (Figs. 4C, 4D) showed a more prominant fluorescence signal compared to that in the shMDMX cells. To further confirm the target specificity, flow cytometry was conducted (Figs. 4C, 4D, right). After cells were incubated with PD_1-BD_2, the fluorescence intensities were higher than that of the control and the shMDMX groups, and were comparable with that of the cells incubated with PD_1 (positive control). This indicates that the PD_1-BD_2 had been activated by the MDMX mRNA of cells. It suggests that the gene-specific drug may be used as an efficient candidate for the MDMX high-expressed cell imaging and killing.

Cellular Cytotoxicity Analysis of PD_1-BD_2

To verify the cytotoxic ROS release of PD_1-BD_2 in cells based on the specific activation by MDMX mRNA, cytotoxicity analysis with CCK8 was implemented. The viabilities of Y79 cells were evaluated by preincubating with an escalating PD_1-BD_2 concentration. The result indicates no significant decrease in cell viability in the cells with only laser and only PD_1-BD_2. Furthermore, 72% ± 1.2% cell lethality was reached with PD_1-BD_2 concentration at 0.6 μM 72 hours incubation after the

laser irradiation (Fig. 5A). The medium drug concentration was then used to demonstrate the flexibility of using light dosage to control the PDT cytotoxicity. By using 0.6 μM drug concentration with an increased laser fluence, cell viabilities decreased to 7.7% ± 1% at 50 J cm^{-2} (Fig. 5B).

Too strong PDT dosage would trigger cell necrosis but apoptosis, resulting in many side effects. The crucial factors in determining the type of cell death following PDT include cell type, light dose, photosensitizer concentration, and its subcellular localization.[35,36] Therefore, a moderate dosage in PDT, 0.6 μM drug and 30 J cm^{-2} laser, was preferred in our experiment.

Y79 cells were irradiated with laser in the presence of PD_1-BD_2, PD_1, and PPa (0.6 μM), then the photodynamic toxicity was assessed after a 48-hour incubation with consideration of the previous MDMX knockdown efficiency. The results show that the viability of Y79 cells treated with PD_1-BD_2 decreased by 68% ± 1.3%, being comparable to both the PD_1 and PPa groups. This indicates that the PPa molecules on PD_1-BD_2 had been activated by MDMX mRNA in cells and retained its efficiency in generating cytotoxicity during laser irradiation. In comparison, the treatment had a significantly lower cytotoxicity on the shMDMX Y79 cells. This clearly demonstrates the effectiveness of the modality on the MDMX high expression Y79 cells (Fig. 5C). A comparison of cell viabilities among Y79, WERI-Rb1, and D407 cells was further implemented. In the results, PD_1-BD_2 exhibited significant killing effect on either Y79 and WERI-Rb1 cells (Fig. 5D). The cells with high expressed MDMX mRNA were more sensitive to PD_1-BD_2-based PDT due to its idiotype.

In order to confirm whether the apoptosis was the prominent cell death mode in the PDT, quantification of apoptosis and necrosis with Annexin V/PI staining and FACS analysis was performed. Figure 6 shows Y79 and WERI-Rb1 cell death mainly through apoptosis in the PD_1-BD_2+laser groups. This observation confirms that with the investigated treatment protocol, apoptosis was a major contribution to the cell death.

Therefore, the PD_1-BD_2 beacons can be triggered by the endogenetic MDMX mRNA and generated cytotoxicity to induce cell apoptosis. The specific mRNA trigging would improve the killing efficiency to retinoblastoma cells and greatly decrease the toxicity to normal cells.

Conclusions

In summary, this work demonstrates the synthesis of a sensitive and effective MDMX mRNA-triggered photodynamic molecular beacon for retinoblastoma therapy. The beacon showed an efficient imaging capability on retinoblastoma cells and resulted in an increased cell apoptosis after PDT in vitro. The properties make it a potential tumor-specific drug for imaging and therapy in the future. The protocol is prospective to be used as a versatile method to design other tumor mRNA-based PDT agent assemblies.

Acknowledgments

The authors thank Junyang Zhao Beijing (Tongren Eye Centre, Beijing Ophthalmology & Visual Sciences Key Lab, Tongren Hospital, Capital Medical University) for providing data analysis assistance.

Supported by the National Natural Science Foundation of China (91539127; 61361160414; 81371646), the Guangdong Natural Science Foundation (2015A030313394), Science and Technology Planning Project (2014A020212738) of Guangdong, and the Science Technology Program Guangzhou (201607010371).

Disclosure: **Y. Wei**, None; **C. Lu**, None; **Q. Chen**, None; **D. Xing**, None

References

1. Zhao J, Dimaras H, Massey C, et al. Pre-enucleation chemotherapy for eyes severely affected by retinoblastoma masks risk of tumor extension and increases death from metastasis. *J Clin Oncol*. 2011;29:845–851.
2. American Brachytherapy Society–Ophthalmic Oncology Task Force. The American Brachytherapy Society consensus guidelines for plaque brachytherapy of uveal melanoma and retinoblastoma. *Brachytherapy*. 2014;13:1–14.
3. Bartuma K, Pal N, Kosek S, Holm S, All-Ericsson C. A. 10-year experience of outcome in chemotherapy-treated hereditary retinoblastoma. *Acta Ophthalmologica*. 2014;92:404–411.
4. Elmore S. Apoptosis: a review of programmed cell death. *Toxicologic Pathology*. 2007;35:495–516.
5. Rivellese MJ, Baumal CR. Photodynamic therapy of eye diseases. *J Ophthal Nursing Technol*. 2000;19:134–141.
6. Walther J, Schastak S, Dukic-Stefanovic S, Wiedemann P, Neuhaus J, Claudepierre T. Efficient photodynamic therapy on human retinoblastoma cell lines. *PLoS One*. 2014;9:e87453.
7. Cerman E, Cekic O. Clinical use of photodynamic therapy in ocular tumors. *Survey Ophthalmol*. 2015;60:557–574.
8. Teixo R, Laranjo M, Abrantes AM, et al. Retinoblastoma: might photodynamic therapy be an option? *Cancer Metastasis Rev*. 2015;34:563–573.
9. Wilson BC, Patterson MS. The physics biophysics and technology of photodynamic therapy. *Phys Med Biol*. 2008; 53:R61–109.
10. Rong P, Yang K, Srivastan A, et al. Photosensitizer loaded nanographene for multimodality imaging guided tumor photodynamic therapy. *Theranostics*. 2014;4:229–239.
11. Wei Y, Song J, Chen Q, Xing D. Enhancement of photodynamic antitumor effect with pro-oxidant ascorbate. *Lasers Surg Med*. 2012;44:69–75.
12. Aiguo Zhou YW, Qun Chen, Da Xing. In vivo near-infrared photodynamic therapy based on targeted upconversion nanoparticles. *J Biomed Nanotechnol*. 2015;11:1–8.
13. Kim JY, Choi WI, Kim M, Tae G. Tumor-targeting nanogel that can function independently for both photodynamic and photothermal therapy and its synergy from the procedure of PDT followed by PTT. *J Control Release*. 2013;171:113–121.
14. Selbo PK, Weyergang A, Eng MS, et al. Strongly amphiphilic photosensitizers are not substrates of the cancer stem cell marker ABCG2 and provides specific and efficient light-triggered drug delivery of an EGFR-targeted cytotoxic drug. *J Control Release*. 2012;159:197–203.
15. Mironova KE, Proshkina GM, Ryabova AV, et al. Genetically encoded immunophotosensitizer 4D5scFv-miniSOG is a highly selective agent for targeted photokilling of tumor cells in vitro. *Theranostics*. 2013;3:831–840.
16. Laurie NA, Donovan SL, Shih CS, et al. Inactivation of the p53 pathway in retinoblastoma. *Nature*. 2006;444:61–66.
17. Garcia D, Warr MR, Martins CP. Brown Swigart L, Passegue E Evan GI. Validation of MdmX as a therapeutic target for reactivating p53 in tumors. *Genes Dev*. 2011;25:1746–1757.
18. Gilkes DM, Chen L, Chen J. MDMX regulation of p53 response to ribosomal stress. *Embo J*. 2006;25:5614–5625.
19. Gilkes DM, Pan Y, Coppola D, Yeatman T, Reuther GW, Chen J. Regulation of MDMX expression by mitogenic signaling. *Mol Cell Biol*. 2008;28:1999–2010.
20. Bo MD, Secchiero P, Degan M, et al. MDM4 (MDMX) is overexpressed in chronic lymphocytic leukaemia (CLL) and marks a subset of p53 wild-type CLL with a poor cytotoxic response to Nutlin-3. *Br J Haematol*. 2010;150:237–239.

Investigative Ophthalmology & Visual Science

21. Tabe Y, Sebasigari D, Jin L, et al. MDM2 antagonist nutlin-3 displays antiproliferative and proapoptotic activity in mantle cell lymphoma. *Clin Cancer Res*. 2009;15:933–942.
22. Laurie NA, Shih CS, Dyer MA. Targeting MDM2 and MDMX in retinoblastoma. *Curr Cancer Drug Targets*. 2007;7:689–695.
23. Lovell JF, Liu TW, Chen J, Zheng G. Activatable photosensitizers for imaging and therapy. *Chem Rev*. 2010;110:2839–2857.
24. Zheng G, Chen J, Stefflova K, Jarvi M, Li H, Wilson BC. Photodynamic molecular beacon as an activatable photosensitizer based on protease-controlled singlet oxygen quenching and activation. *Proc Natl Acad Sci U S A*. 2007;104:8989–8994.
25. Liu TW, Akens MK, Chen J, Wise-Milestone L, Wilson BC, Zheng G. Imaging of specific activation of photodynamic molecular beacons in breast cancer vertebral metastases. *Bioconjug Chem*. 2011;22:1021–1030.
26. Lo PC, Chen J, Stefflova K, et al. Photodynamic molecular beacon triggered by fibroblast activation protein on cancer-associated fibroblasts for diagnosis and treatment of epithelial cancers. *J Med Chem*. 2009;52:358–368.
27. Gao Y, Qiao G, Zhuo L, Li N, Liu Y, Tang B. A tumor mRNA-mediated bi-photosensitizer molecular beacon as an efficient imaging and photosensitizing agent. *Chem Commun (Camb)*. 2011;47:5316–5318.
28. Arian D, Clo E, Gothelf KV, Mokhir A. A nucleic acid dependent chemical photocatalysis in live human cells. *Chemistry*. 2010;16:288–295.
29. Clo E, Snyder JW, Voigt NV, Ogilby PR, Gothelf KV. DNA-programmed control of photosensitized singlet oxygen production. *J Am Chem Soc*. 2006;128:4200–4201.
30. Lovell JF, Chen J, Huynh E, Jarvi MT, Wilson BC, Zheng G. Facile synthesis of advanced photodynamic molecular beacon architectures. *Bioconjug Chem*. 2010;21:1023–1025.
31. Verhille M, Couleaud P, Vanderesse R, Brault D, Barberi-Heyob M, Frochot C. Modulation of photosensitization processes for an improved targeted photodynamic therapy. *Curr Med Chem*. 2010;17:3925–3943.
32. Liu TW, Chen J, Burgess L, et al. Activation kinetics of zipper molecular beacons. *J Phys Chem B*. 2015;119:44–53.
33. Wei Y, Zhou J, Xing D, Chen Q. In vivo monitoring of singlet oxygen using delayed chemiluminescence during photodynamic therapy. *J Biomed Opt*. 2007;12:014002.
34. Wang J, Xing D, He Y, Hu X. Experimental study on photodynamic diagnosis of cancer mediated by chemiluminescence probe. *FEBS Lett*. 2002;523:128–132.
35. Castano AP, Demidova TN, Hamblin MR. Mechanisms in photodynamic therapy: part two-cellular signaling, cell metabolism and modes of cell death. *Photodiagn Photodyn Ther*. 2005;2:1–23.
36. Plaetzer K, Kiesslich T, Verwanger T, Krammer B. The modes of cell death induced by PDT: an overview. *Med Laser Appli*. 2003;18:7–19.

Investigative Ophthalmology & Visual Science